POSSIBLE BEAM QUALITY OF THE ANTIPROTONS IN THE HESR

A.Dolinskii[1],A.Bolshakov[2], O.Boine-Frankenheim[1], B.Franzke[1],
M.Steck[1],A.Sidorin[3], G.Trubnikov[3], P.Zenkevich[2]
1 – GSI, Darmstadt, Germany ,2 – ITEP Moskow, Russia, , 3 - JINR, Dubna, Russia,

Abstract

In this article some numerical calculations that have been done in order to evaluate the equilibrium beam emittances and momentum spreads at the high energy of antiprotons in the HESR are outlined. The aim of this study is to find out the optimal value between the reasonable parameters of the e-cool system and required luminosity and desired beam properties during experiment where strong electron cooling is to be applied.....

1 INTRODUCTION

A new accelerator facility is being designed at GSI for operation with heavy ion beams as well as for production, cooling and accumulation of antiprotons [1]. The main installation for experiments with antiprotons will be the high energy storage ring HESR [2] that allows storage of antiprotons in the energy rangy 0.8 to 15 GeV. Luminosity of up to 2×10^{32} $cm^{-2}s^{-1}$ is expected for experiments with an internal hydrogen target. The high-energy electron cooling of antiproton beams is considered to provide antiproton beams of high quality. The main goal of this work is to find out the achievable antiproton beam quality in the HESR. The high luminosity together with a high beam quality is possible only if fast electron cooling can be employed. One has to take into account the reasonable electron beam parameters of the e-cooler and beta-functions in the HESR at which the high intensity and high quality of the pbar beam can be obtained. Three main effects (electron cooling, beam heating by IBS and target effects) that are influence on the quality of the circulated beam are considered.

The antiproton beam quality and the average luminosity in the HESR will be limited by achievable cooling rate and the capability to suppress heating processes by IBS and internal target. Obviously, strong cooling can only be achieved by the so-called magnetised cooling requiring a strong longitudinal magnetic field (B=0.5 T) that guides the electron beam along the entire interaction region.....

2 THE TOOLS FOR CALCULATIONS

The equilibrium between electron cooling, IBS and target heating has been calculated by three different codes (BETACOOL, MOCAC and PTARGET), where the different algorithms for calculation of the mentioned main effects are applied.

BETACOOL [3,4] program was developed by Meshkovs group to calculate the evolution of the ion beam parameters taking into account the electron cooling process. In this code the IBS growth rates using ring lattice function imported from output file of the MAD program is included. One can calculate the equilibrium between electron cooling, IBS and internal target heating (only jet target). The algorithm of the problem analysis consists in the solution of the equation for root mean square values of the beam phase volumes of three degrees of freedom. The program structure is designed in such a way that permits to include into calculation any process separately, which can be described with cooling or heating rates.

MOCAC [5,6] (MOnte CArlo Code) was developed by A.Bolshakov and P.Zenkevich, where one can calculate the evolution of the ion beam by direct modelling of beam dynamic

by Monte-Carlo method of co-called 'big particles'. The main processes that are considered in this code are interaction of the ion beam with electrons of the cooling system, intra-beam scattering, interaction with internal target (only jet target), space charge effects (ion and electrons in e-cool). Here the ensemble of particles with arbitrary initial distribution in 3-dimensional phase space is considered and then the interactions of each process inside this ensemble are calculated. The simulation is performed by method of co-called "big events", where the time τ of all interaction is parameter of calculation. This time parameter must be much less then typical time of changing the main beam parameters T. The minimum τ can be equal the time which is needed for particles to make one turn in the ring. But in this case the calculation takes rather long time. One has to find optimal value of the τ in order to have a stable solution of the task and at the same time to have a fast time of simulation.

PTARGET (Pellet TARGET) was developed by Franzke's group to investigate the beam dynamic evolution in the HESR taking into account the cooling effect, IBS, and heating of the ion beam by a pellet target. In this code the Monte Carlo modelling is applied to evaluate the emittance and the momentum spread depending on time. Here any number of the particles can be generated with a gaussian momentum distribution and a gaussian density probability in the (x,x',y,y') phase space. For calculations the storage ring is not considered in detail, only the phase advances between internal target and electron cooling system and Twiss parameters on these elements are taken into account. The particles parameters are calculated from turn to turn, where the cooling effects and heating of the beam by IBS and pellet target take place.

2.1 Modelling of The Electron Cooling

Modelling of the electron cooling process in MOCAC code is based on binary collisions between ion and electrons in a laboratory reference frame, where the analysis of ion motion is considered. Let us introduce some vector u, whose components are defined by:

$$u_1 = \frac{1}{\gamma}\frac{\Delta p}{p}, u_2 = x', u_3 = y' . \qquad 1$$

Here Δp is the ion momentum deviation, x, y are horizontal and vertical coordinates of the ion, x', y' are corresponding derivatives over longitudinal variable s.

For classical binary collisions model (CBCM) in these variables equation of motion can be written as follows:

$$\frac{du_i}{dt} = -2AL_C(\theta)\frac{u_i - u_e}{\theta^3} \qquad 2$$

where $u_{i,e}$ corresponds to ion and electron velocity, $\theta = |u_i - u_e|$. In a presence of space charge effects $u_e = u_{sc} + \Delta u_e$, where u_{sc} is a space charge component of the electron velocity, Δu_e is a random one,

$$A = f\frac{2\pi r_i r_e c n_e}{\beta^3\gamma^5} \qquad 3$$

In Eq.(3) constant $f=l_{lool}/l_{ring}$ (l_{cool} is the cooler length, l_{ring} is the ring circumference), r_e, r_p are electron and proton classical radii, n_e the electron density inside the cooler, c is light speed, β,γ are relativistic parameters. After averaging on the electron random velocities we can write Eq.(2) in the following form:

$$\frac{du}{dt} = 2A\overset{\circ}{F}_{fr}(\overset{\circ}{U}) \qquad 4$$

where $F_{fr}(U)$ is "dimensionless friction force", $U = \check{u}_i - \check{u}_{sc}$. This friction force can be calculated analytically only for constant value of Coulomb logarithm and the simplest case of Maxwellian distribution. Usually the longitudinal temperature is much less than the transverse one and for the corresponding "flattened" particles distribution the exact integration can be done only numerical that is performed in MOCAC and BETACOOL codes in case of nonmagnetized electrons.

In case of magnetized electron the cooling rates are calculated in BETACOOL and MOCAC codes through averaging of action of the friction force inside the electron cooler over phases of betatron and synchrotron oscillations and over Gaussian distribution function of the particles in the space of the motion invariants.

Binary collisions model for partially magnetized electrons is based on separation of three regions in relative electron-ion velocities v : 1) region H (high particle velocities), where $v > \Delta_\perp$, 2) region L (low particle velocities), where $\Delta_\parallel < v < \Delta_\perp$; 3) region S (super low particle velocities), where $v < \Delta_\parallel$. Here $\Delta_\parallel$ and $\Delta_\perp$ are respectively electron velocities in longitudinal and transversal directions and defined by the longitudinal and transverse rms electron temperature spread at the output of a cathode:

$$\Delta_\perp = \sqrt{\frac{kT_\perp}{m_e}}\ , \quad \Delta_{\text{II}} = \sqrt{\frac{kT_{\text{II}}}{m_e}}\ , \tag{5}$$

m_e is the electron masse, k is Boltzmann constant, T is a temperature.

All collisions depending on the region and the impact parameter are divided on three kinds: 1)"classical fast" collisions with very low impact parameter where magnetic field does not influence on the process; 2) multiple interaction with impact parameter near the radus of the Larmor rotation; 3)"slow" interactions at distances essentially larger than the Larmor radius. Resulting formulae for friction force are given in [7] (formulae Derbenev-Skrinsky):

$$\overset{\circ}{F}_\perp \approx -\frac{2\pi n_e Z_i e^4}{4\pi\varepsilon_0 m_e}\overset{\circ}{v}_\perp \begin{cases} \dfrac{1}{v^3}\left(2L_{H1} + \dfrac{v_\perp^2 - 2v_{\text{II}}^2}{v^2}L_{H2}\right), \ldots\ldots\ldots\ldots H \\ \dfrac{2}{\Delta_\perp^3}\left(L_{L1} + N_1 L_{L2}\right) + \dfrac{v_\perp^2 - 2v_{\text{II}}^2}{v^2}\dfrac{L_{L3}}{v^3}, \ldots L \\ \dfrac{2}{\Delta_\perp^3}\left(L_{S1} + N_2 L_{S2}\right) + \dfrac{L_{S3}}{\Delta_{\text{II}}^3}, \ldots\ldots\ldots\ldots S \end{cases} \tag{6}$$

$$\overset{\circ}{F}_{\text{II}} \approx -\frac{2\pi n_e Z_i e^4}{4\pi\varepsilon_0 m_e}\overset{\circ}{v}_{\text{II}} \begin{cases} \dfrac{1}{v^3}\left(2L_{H1} + \dfrac{3v_\perp^2}{v^2}L_{H2} + 2\right), \ldots\ldots\ldots\ldots\ldots\ldots H \\ \dfrac{2}{\Delta_\perp^2\Delta_{\text{II}}}\left(L_{L1} + N_1 L_{L2}\right) + \left(\dfrac{3v_\perp^2}{v^2}L_{L3} + 2\right)\dfrac{1}{v^3}, \ldots L \\ \dfrac{2}{\Delta_\perp^2\Delta_{\text{II}}}\left(L_{S1} + N_2 L_{S2}\right) + \dfrac{L_{S3}}{\Delta_{\text{II}}^3}, \ldots\ldots\ldots\ldots\ldots S \end{cases} . \tag{7}$$

$v_\parallel$, $v_\perp$ are the longitudinal and transversal vector components of the v ion velocity (in a system accompanying the electron beam) along and perpendicular to the magnetic field respectively; e, m_e are electron charge and mass; ε_0 is the permitivity constant of free space; Z_i is the ion charge; N_1, N_2 are number of multiple collisions; n_e is the electron beam density:

$$n_e = \frac{I_e}{e\beta c\pi a_e^2}, \qquad 8$$

where I_e is the electron current, a_e is the electron beam radius. The Coulomb logarithms for each region are the following:

For high particle velocities $v>\Delta_\perp$:

$$L_{H1} = \ln\left(\frac{m_e v^3}{Z_i e^2 \omega_B}\right) \approx 10 - \ln Z_i,$$

$$L_{H2} = \ln\left(\frac{v\omega_B}{2\Delta_\perp \omega_{pe}}\right) \approx 2.$$

For low particle velocities $\Delta_{II} < v < \Delta_\perp$:

$$L_{L1} = \ln\left(\frac{m_e v^3}{Z_i e^2 \omega_B}\right) \approx 5 - \ln Z_i,$$

$$L_{L2} = \ln\left(\frac{2\Delta_\perp}{\Delta_\perp \to \Delta_{II}}\right) \approx 0.7 \to 4,$$

$$L_{L1} = \ln\left(\frac{\min\left\{\left(v/\omega_{pe}\right), \left(3Z_i/n_e\right)^{\frac{1}{3}}\right\}_B}{2\left\langle \rho_\perp \right\rangle}\right) \approx 3 - 1.$$

For super low particle velocities $v < \Delta_{||}$:

$$L_{S1} = \ln\left(\frac{m_e \Delta_{II} \Delta_\perp^2}{Z_i e^2 \omega_B}\right) \approx 5 - \ln Z_i,$$

$$L_{S2} = \ln\left(\frac{2\Delta_\perp}{\Delta_{II}}\right) \approx 5,$$

$$L_{S3} = \ln\left(\frac{1}{2\left\langle \rho_\perp \right\rangle}\left(\frac{3Z_i}{n_e}\right)^{\frac{1}{3}}\right) \approx 2.$$

where $\rho_\perp$ is the Larmor radius of electron, ρ_{min} is a minimal impact parameter, ω_{pe} is the electron beam plasma frequency, $\omega_B = eB/(\gamma m_e c)$, c is the speed of light.

This collection of the formulas shows how complicated the dependence of the friction force on the parameters of the Coulomb logarithms. In PTARGET code the interpolated expressions of the friction forces for the electron cooling are applied to make the calculation more fast because the interactions of the particles with internal target and e-cool are calculated from turn to turn. In this code the longitudinal and transversal force components in all particle velocity regions are approximately expressed by the following formulae [6]:

$$F_\perp = -\frac{2\pi n_e Z_i e^4 L_c}{4\pi\varepsilon_0 m_e}\frac{v_\perp}{v^3}\left(2L_1 + \frac{v_\perp^2 - 2v_{II}^2}{v^2}L_2\right), \qquad 9$$

$$F_{II} \approx -\frac{2\pi n_e Z_i e^4 9 L_c}{4\pi\varepsilon_0 m_e}\left(\frac{v_\perp^2 v_{II}}{6v^5 + \Delta_{II}^3 v_\perp^2}\right), \qquad 10$$

where

$$v = \sqrt{v_\perp^2 + v_{II}^2}, \quad v_\perp = \gamma_0 \beta_0 c \theta_\perp, \quad v_{II} = \beta_0 c \frac{\Delta p}{p}, \quad \theta_\perp = \sqrt{\frac{\varepsilon}{\beta_{cool}}},$$

ε is the transversal emittance, β_{cool} is the beta function in the electron cooling system, $\Delta p/p$ is the momentum deviation of the particle. The Coulomb logarithms L_c, L_1, L_2 are assumed constants and used as parameters to fit one time the shape of forces as close as possible to the forces that are calculated by formulae 2, 3.

2.2 Intra-beam scattering (IBS).

Intra-beam scattering is a multiple Coulomb scattering of charged particles in a beam. It causes small changes of momentum of colliding particles and leads to a continuous increase of bunch or beam dimensions and to a reduction of the beam lifetime when the particle hit the aperture. In MOCAC code the binary collisions model is used for modeling of this effect. The momentum of two colliding particles before the collision are given by

$$\overset{\circ}{p}_{1,2} = \begin{pmatrix} p_{s1,2} \\ p_{x1,2} \\ p_{1,2} \end{pmatrix} \qquad 11$$

In order to determine the changes of the two momentums due to collision we transform the momentum into the center-of-mass system where they have opposite directions but the same absolute value. Due to the collision their directions are changes by the azimuths angle ψ and by the polar angle ϕ whereas their absolute value remains constant. The changed momentum can then be transformed back into the laboratory system. The momentum change can be written in the form

$$\delta\overset{\circ}{p}_{1,2} = \pm\frac{p}{2}\begin{pmatrix} \gamma\chi\cos\phi\sin\psi + \gamma\xi(\cos\psi - 1) \\ \frac{1}{\chi}(\zeta\rho\sin\phi - \theta\xi\cos\phi)\sin\psi + \theta(\cos\psi - 1) \\ \frac{1}{\chi}(-\theta\rho\sin\phi - \zeta\xi\cos\phi)\sin\psi + \zeta(\cos\psi - 1) \end{pmatrix} \qquad 12$$

where

$$\xi = \frac{p_1 - p_2}{\gamma p}, \quad \theta = \frac{p_{x1} - p_{x2}}{p}, \quad \zeta = \frac{p_{y1} - p_{y2}}{p} \quad \chi^2 = \theta^2 + \zeta^2, \quad \rho^2 = \xi^2 + \theta^2 + \zeta^2,$$

p is the mean particle momentum and γ is the mean particle energy divide by its rest energy. The probability for the scattering into a solid angle determined by $d\psi$ and $d\phi$ is given by the Rutherford cross-section in the center-of-mass system

$$d\sigma = \left(\frac{r_p}{4\beta^2 \sin^2\frac{\psi}{2}}\right)^2 \sin\psi d\psi d\phi \quad , \qquad 13$$

where r_p is the classical proton radius. The minimum scattering angle ψ_{min} is determined by the maximum impact parameter d in the center-of-mass system:

$$\tan\frac{\psi_{\min}}{2} = \frac{r_p}{2d\beta^2} \qquad 14$$

d gives a cut-off angle for ψ which is rather arbitrary, but its influence on the results is weak. We assume d=min(h,r_d), where h is chamber half height, r_d is Debye radius. Using formulae 12 and 13 we can calculate the results of the "individual" binary collision. We consider the discrete random process as a sequence of "equivalent" scattering events with scattering angle Ψ_{eff} which is defined by:

$$\Psi_{eff} = \frac{2\sqrt{\pi}\,r_i}{\left(\overline{\beta}^{3/2}\gamma\right)}\sqrt{c\cdot\rho\cdot\delta t\cdot\ln\frac{2d\overline{\beta^2}}{r_i}}\ ,$$

where ρ is the local density of the beam in the laboratory frame, δt- time interval.

In BETACOOL the two modes for the calculations of IBS growth rate can be used in the present version of the program (Martini and Piwinski). To calculate IBS with the Martini model one needs to use the lattice functions of the MAD code for different modes of its operation. In accordance with the Martini model the growth rates can be inserted into the code in the form of the corresponding characteristic times [10]:

$$\begin{aligned}\frac{1}{\tau_p} &= \left\langle \frac{nA}{2}\left(1-d^2\right)f_1 \right\rangle \\ \frac{1}{\tau_{x'}} &= \left\langle \frac{A}{2}\left[f_2+\left(d^2+\tilde{d}^2\right)f_1\right] \right\rangle \\ \frac{1}{\tau_{z'}} &= \left\langle \frac{A}{2}f_3 \right\rangle\end{aligned} \qquad 15$$

where angular brackets mean averaging over the ring circumference, n = 1 for a bunched beam and n = 2 for coasting beam,

$$A = \frac{\sqrt{1+\alpha_x^2}\sqrt{1+\alpha_z^2}\,cr_i^2\lambda}{16\pi\sqrt{\pi}\sigma_{x_\beta}\sigma_{x'_\beta}\sigma_z\sigma_{z'}\sigma_p\beta^3\gamma^4}$$

λ is the linear ion density:

$$\lambda = \begin{cases} N/L, & \textit{for coasting beam} \\ N_b/\left(2\sqrt{\pi}\sigma_s\right), & \textit{for a bunched beam} \end{cases}.$$

The functions f_i are integrals of the following form:

$$f_i = k_i\int_0^\infty\int_0^\pi\int_0^{2\pi}\sin\mu\, g_i(\mu,\nu)\exp\left[-D(\mu,\nu)z\right]\ln\left(1+z^2\right)d\nu d\mu dz\ , \qquad 16$$

with the coefficients $k_1 = 1/c^2$, $k_2 = a^2/c^2$, $k_3 = b^2/c^2$, and

$$D(\mu,\nu) = \frac{1}{c^2}\left[\sin^2\mu\cos^2\nu + \sin^2\mu\left(a\sin\nu - \tilde{d}\cos\nu\right)^2 + b^2\cos^2\mu\right],$$

$$g_1(\mu,\nu) = 1 - 3\sin^2\mu\cos^2\nu\,,$$

$$g_2(\mu,\nu) = 1 - 3\sin^2\mu\sin^2\nu + 6\tilde{d}\sin^2\mu\sin\nu\cos\nu/a\,,$$

$$g_3(\mu,\nu) = 1 - 3\cos^2\mu\,.$$

The normalised parameters are to be calculated from the following expressions:

$$a = \frac{\sigma_y}{\sigma_{x'_\beta}}\sqrt{1+\alpha_x^2}\,,\ b = \frac{\sigma_y}{\sigma_{z'}}\,,\ c = q\sigma_y\,,\ d = \frac{\sigma_p}{\sigma_x}D\,,\ \tilde{d} = \frac{\sigma_p}{\sigma_x}\tilde{D}\,,$$

where $\tilde{D} = \alpha_x D + \beta_x D'$, $\sigma_x^2 = \sigma_{x_\beta}^2 + D^2\sigma_p^2$, $\sigma_y = \dfrac{\sigma_p\sigma_{x_\beta}}{\gamma\sigma_x}$ and $q = 2\beta\gamma\sqrt{\dfrac{\sigma_z}{r_i}}$.

The integration 16 over all variables is performed numerically.

In PTARGET code the Piwinski model is applied [11,12]. To have a fast calculation the IBS is considered in a smooth focusing approximation and only IBS rates are calculated from turn to turn depending on the Gaussian distribution of the particles in the beam. The IBS increments average over the Gaussian particles distribution in a coasting beam are expressed by formulae

$$\tau_x^{-1} = F\left[\left(\frac{\gamma^2}{Q_x} + \frac{1}{2}\right)\frac{\arctan(\sqrt{x-1})}{\sqrt{x-1}} - \frac{\frac{\gamma^2}{Q_x^2} - \frac{1}{2}}{x-1}\left(1 - \frac{\arctan(\sqrt{x-1}}{\sqrt{x-1}}\right)\right] \qquad 17$$

$$\tau_y^{-1} = \frac{F}{2}\left[\frac{\arctan(\sqrt{x-1})}{\sqrt{x-1}} + \frac{1}{x-1}\left(1 - \frac{\arctan(\sqrt{x-1}}{\sqrt{x-1}}\right)\right] \qquad 18$$

$$\tau_s^{-1} = F\frac{Q_x\gamma^2\varepsilon_x}{R\sigma_s^2}\left[\frac{\arctan(\sqrt{x-1})}{\sqrt{x-1}} - \frac{1}{x-1}\left(1 - \frac{\arctan(\sqrt{x-1}}{\sqrt{x-1}}\right)\right] \qquad 19$$

where parameters F and x denote

$$F = \frac{N_i r_p^2 c L_c}{8\pi\gamma^4\beta^3\varepsilon_x\varepsilon_y\sigma_\delta\sigma_s}\frac{Z_i^2}{A_i}\,,\quad x = \frac{\gamma^2}{Q_x}\left(1 + \frac{\varepsilon_x Q_x^3}{R\sigma_\delta^2}\right),$$

$$\sigma_s = \sqrt{2\pi}R\,,\qquad \sigma_\delta = \frac{\Delta p}{p}\,.$$

N_i is a number of the particles, r_p is the proton classical radius, L_c is a Coulomb logarithm, c is the speed of light, A_i , Z_i are ion atomic mass, charge. $\varepsilon_{x,y}$ is a transversal beam emittance, $Q_{x,y}$ is a tune, R is average ring radius. It should be noted that these formula give a good agreement with experimental results. As an example in Figure 1 one can see comparison between calculated by formulae 17-19 and experimentally measured data for proton beam at the test storage ring TSR [13].

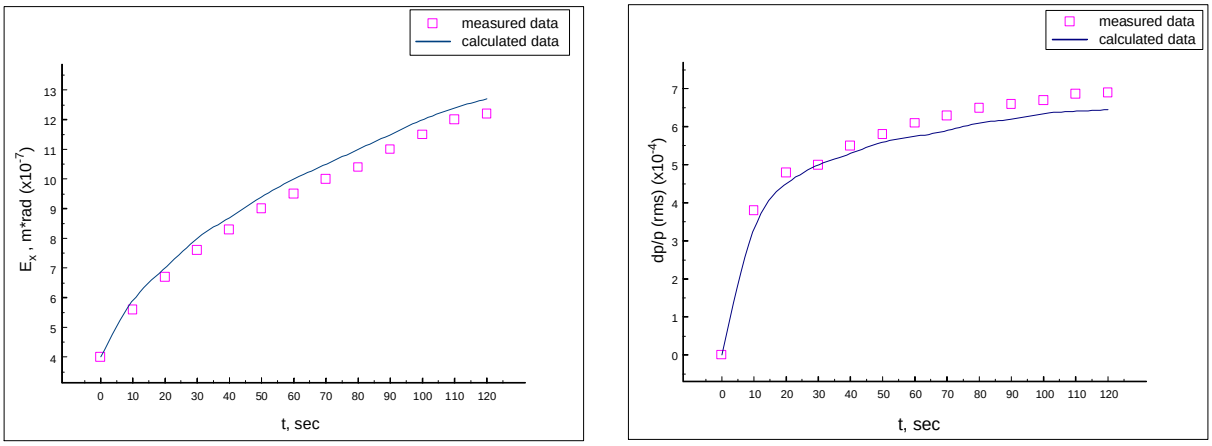

Fig.1 Blow-up of a 10 MeV proton beam of 1×10^9 particles due to IBS at the TSR.

2.3 Target parameters calculation

The planning of internal target experiments in the HESR requires a detailed knowledge of the emittance growth and the beam lifetime. All target effects can be parameterised by two quantities, the mean square values θ_{str} and $\Delta p/p_{\text{target}}$ of the small angle scattering and relative momentum straggling per target traversal. In MOCAC, BETACOOL and PTARGET codes the parameters $\Delta p/p_{\text{target}}$, θ_{str}, are calculated in accordance with the following formulae [14]:

$$\theta_{str}^2 = 2N_t\pi\left(\frac{Z_T Z_P r_e}{\beta c}\right)^2\left[\ln\left(\frac{\alpha_2^2}{\chi^2}\right)-1+\Delta b\right], \qquad 20$$

$$\left(\frac{\Delta p}{p}\right)^2_{target} = \left(\frac{\gamma}{\gamma+1}\right)^2\frac{E_{str}^2}{E^2}, \qquad 21$$

Here, N_t is the number of targets atoms per unit area, Z_P and Z_T are the charge number of projectile and target atoms, p and E is the particle momentum and kinetic energy, r_e is the electron classic radius.

$$E_{str}^2 = \xi\Delta E_{\max}\left(1-\frac{\beta^2}{2}\right).$$

The parameters α_2, χ and Δb are given by the equations:

$$\alpha_2 = \frac{a}{\left(A_T^{1/3}+A_P^{1/3}\right)r_0},$$

where $\lambda = \hbar / p$ is De Broglie wavelength, A_T and A_P are the mass numbers of the target and the projectile, r_0 = 1.3 fm,

$$\chi^2 = 1.13\alpha_1^2\left[1+3.33\left(\frac{Z_T Z_P}{137\beta}\right)^2\right],$$

where

$$\alpha_1 = \frac{\lambda}{0.885 a_0\left(Z_T^{2/3}+Z_P^{2/3}\right)^{1/2}},$$

$a_0 = 0.529\cdot10^{-8}$ cm denotes the Bohr radius,

$$\Delta b = \frac{1}{Z_T}\left\{\ln\left[\frac{1130\beta^2}{Z_T^{4/3}(1-\beta)^2}\right]-u_{in}-\frac{\beta^2}{2}\right\},$$

where u_{in} is a constant determined by the electron configuration of the target atom (from the Thomas-Fermi model one finds u_{in} = -5.8, for the H-atom exact calculation yields u_{in} = -3.6, for Li- and O-atoms the values of u_{in} are -4.6 and -5.0, respectively). E_{max} is the maximum energy loss in a head-on collision of the projectile with a target electron:

$$E_{\max} = \frac{2m_e c^2\beta^2\gamma^2}{1+2\gamma\frac{m_e}{M}+\left(\frac{m_e}{M}\right)^2},$$

with m_e is the electron mass and M - the projectile mass. ξ is a quantity which is proportional to the area density ρx of the target (ρ – target density in g/cm^3):

$$\xi = 0.1535\frac{MeV\,cm^2}{g}\frac{Z_1^2}{\beta^2}\frac{Z_2}{A_2}\rho x\,.$$

3 COMPARISON OF THE CALCULATED AND EXPERIMENTALLY MEASURED RESULTS

The numerical calculation by MOCAC, BETACOOL and PTARGET codes of the equilibrium beam parameters between IBS and electron cooling were performed for the Experimental Storage Ring (ESR) to make a comparison of the obtained results with its experimentally measured. As an example only two type of ions (*U* and *Ni*) have been considered. Some general parameters of the ESR and the ion are given in Table 1, where one can find also for a convenient some parameters of the electron cooling system which have been used in the simulations.

For calculation only the electron cooling process and IBS have been took into account. The electron cooling in MOCAC and BETACOOL codes was performed with two models of the friction forces – flattened non-magnetised model and Derbenev-Skrinsky formulae 6, 7 (magnetised electron beam). In MOCAC code IBS is considered by binary collisions and in BETACOOL code via Martini model. Both those codes require the real Twiss parameters over the ring. This data were imported from output MAD file for the ESR. In PTARGET code IBS is calculated by Piwinsky formulae 17-19 as it was mentioned previously and simple formulae of the friction forces 9-10 for electron cooling are applied.

Fig.2-3 show the dependence of the ion beam emittance and momentum spread for *U* and *Ni* ion beams as function of the number stored particles under constant cooling condition calculated by MOCAC code. At the same figures the experimentally measured values are plotted as well.

Table 1. Parameters of the Experimental Storage Ring (ESR) with electron cooling.

Circumference, *C*, m	108.4
Magnetic field strength, $B\rho$, T·m	10
Particle energy, *E*, MeV/u	30-560
Type of ion	<238
Length of cooling section, *L*, m	2.5
Beta functions in cooling section: β_{hor}, m β_{ver}, m	16 6.9
Electron beam radius, r, cm	2.5
Electron beam current, I, mA	250
Longitudinal electron temperature, $T_{\|}$, meV	0.2
Transversal electron temperature, $T_{\perp}$, meV	100
Magnetic field of cooling section, *B*, kG	1

In Fig.4, 5 the results of equilibrium beam parameters calculated by BETACOOL code are shown. Here we can see that both the magnetized and nonmagnetized cases for the electron beam give lower values of equilibrium for the ion beam compare to that were obtained experimentally. Even nonmagnetized case roughly agrees better with the experimental data. According to BETACOOL calculation one has found that final equilibrium values strongly depended on cooling conditions specially on the transverse and longitudinal electron temperature.

For comparison between all codes in case of the magnetized electron beam fig.6 shows the results of equilibriums calculated by MOCAC, BETACOOL and PTARGET. It is seen that all codes give more less the same results. In some cases the maximal differences of the equilibrium values are a factor of about 3 between obtained calculated results.

One can see that the measured ion beam temperature is increased with the particle number. This can be well explained with strong IBS in an ion beam of higher intensity. In all experiments (not only with *U* and *Ni*) a $N^{1/3}$ – dependence of the momentum spread on the number of stored particles *N* has been observed. For the transverse emittance results varied in the range $N^{1/3}$ to $N^{2/3}$ [9] indicating a high sensitivity to the actual cooling condition. According to the simulated results one can see that the magnetised electron beam gives strong cooling effect mainly for the momentum spread. But the experimental results are agreed more better with data which were calculated with flattened non-magnetised model for a friction forces. In all cases the experimental results lie somewhere between the data calculated with a magnetised and non-magnetised electron beam. It seems in future it is useful to use both model of the electron cooling to find out at least the boundary of area where the equilibrium beam parameters can be observed experimentally.

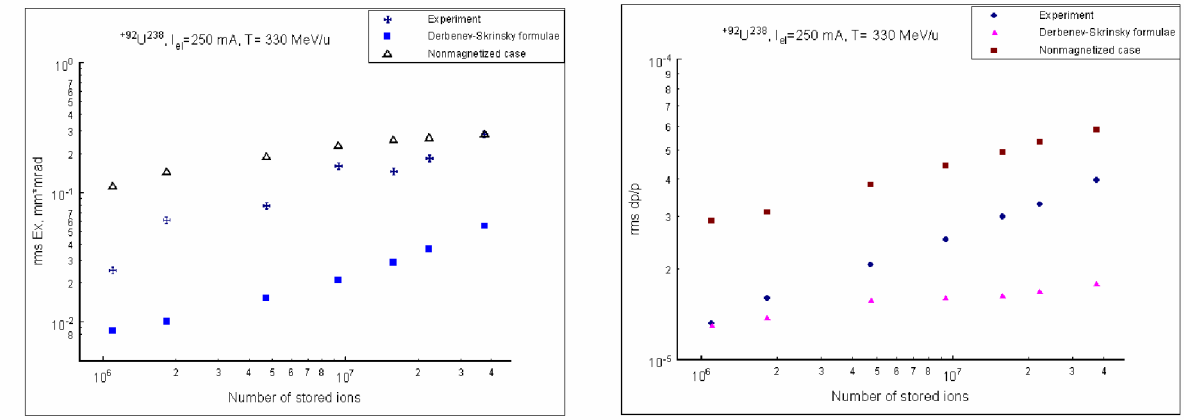

Fig.2 The equilibrium momentum spread and horizontal emittance calculated by MOCAC code.

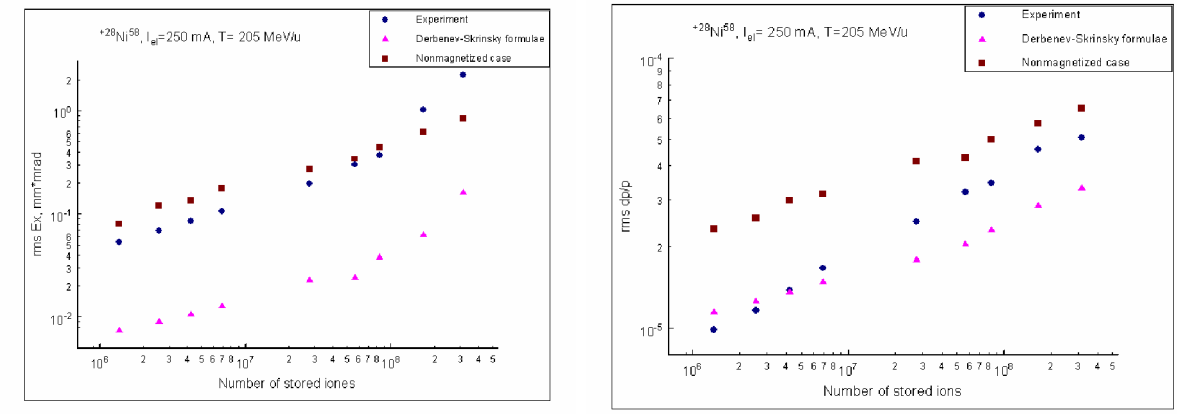

Fig.3 The equilibrium momentum spread and horizontal emittance calculated by MOCAC code.

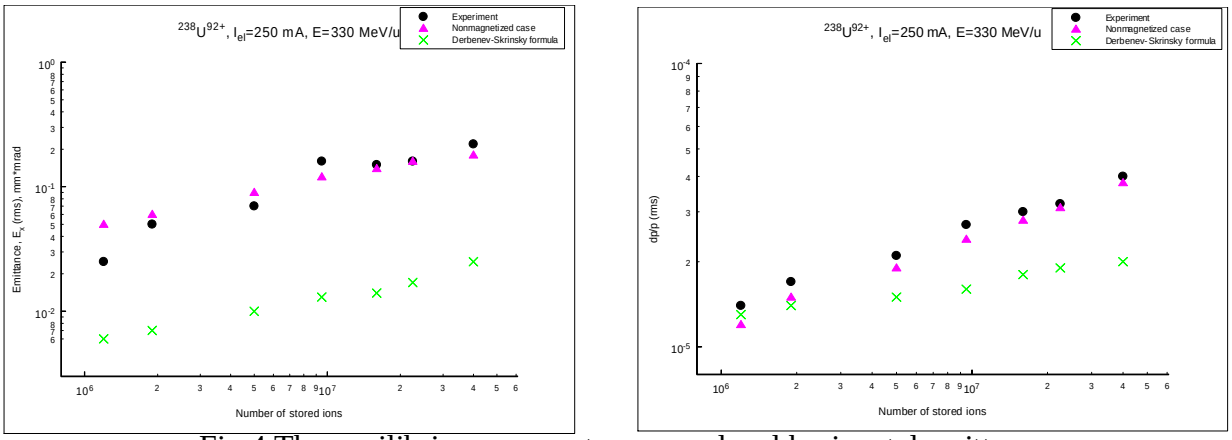

Fig.4 The equilibrium momentum spread and horizontal emittance calculated by BETACOOL code.

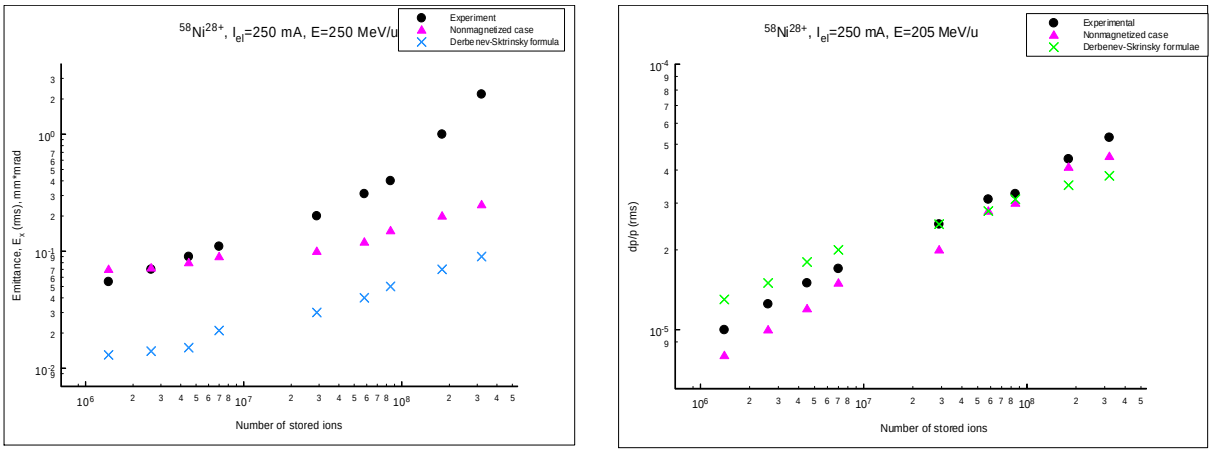

Fig.5 The equilibrium momentum spread and horizontal emittance calculated by BETACOOL code.

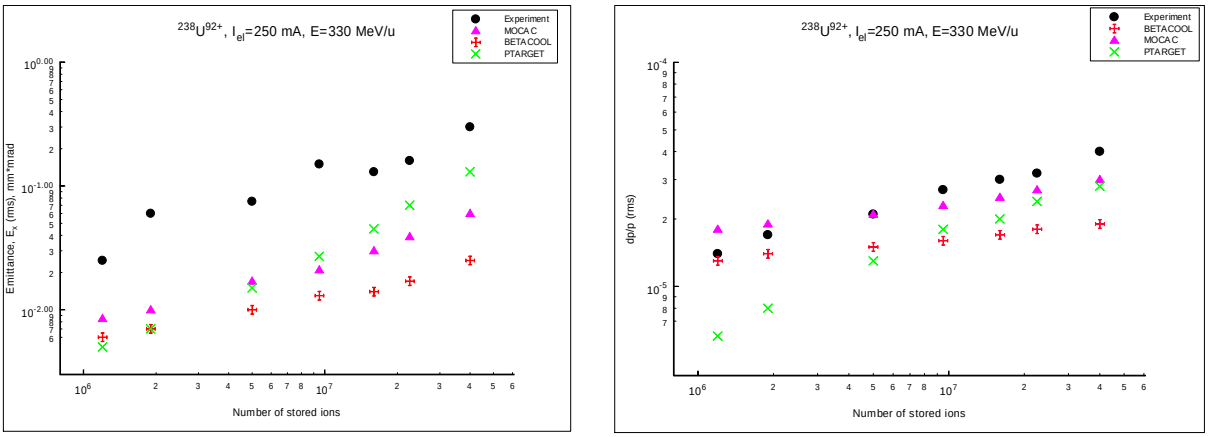

Fig.6 The equilibrium momentum spread and horizontal emittance calculated by MOCAC, BETACOOL, PTARGET codes (‘magnetized’ electron cooling).

4 SIMULATED EQUILIBRIUM BEAM PARAMETERS IN THE HESR

The numerical simulation of the equilibrium beam parameters in the HESR for the antiproton energy range of 0.8-14 GeV were made on computer by MOCAC, BETACOOL and PTARGET codes. As it was mention before, in all of these three codes the different algorithm has been implemented to calculate the evolution of the beam parameters in the ring. It is known that the equilibrium beam parameters are determined through the balance of electron cooling, intrabeam scattering (IBS) and target heating.

At the beginning the equilibrium state between only IBS and electron cooling has been simulated. One can at the same time compare the results, which are obtained by all of these codes. All the needed parameters of the electron cooling system and some general parameters of the HESR, which have been used in simulations, are summarised in the Tables 3, 4.

Table 3. Parameters of the HESR, electron cooling system and initial beam parameters.

Circumference, C, m	430.4
Magnetic field strength, BR, Tm	50
Particle energy, E, GeV	0.8-14.5
Type of ion	Antiproton
Transversal emittance (normalised at injection), $\varepsilon_{\perp}$	2 mm·mrad
Momentum spread (at 1 GeV), $\Delta p/p$	$\pm 4\times10^{-4}$
Number of particles, N_i	5×10^{10}
Gamma-tr, γ_{tr}	19.72
Tune, Q_x Q_y	10.67 8.17

Table 4. Parameters of the electron cooling system.

Electron energy range, E, MeV	0.5-1.5
Electron current, I, mA	250
Electron beam radius, r, cm	2.5
Magnetic field strength, B, kGs	5
Length of cooling section, L, m	30
Beta functions in cooling section: β_{hor}, m β_{ver}, m	190 190
Electron density, n_e , cm^{-3}	10^6
Longitudinal electron temperature, $T_{\parallel}$, meV	0.2
Transversal electron temperature, $T_{\perp}$, meV	100

Fig.7 shows the results of calculation by MOCAC and BETACOOL codes with non-magnetized electron cooling and Fig.8 the equilibrium calculated by all three codes in case of magnetized electron cooling for two different antiproton energies of 1 and 6 GeV. All codes give more less the same results and tendency of reduction of equilibrium states with increasing energy. That means the heating by IBS with energy increasing is reduced.

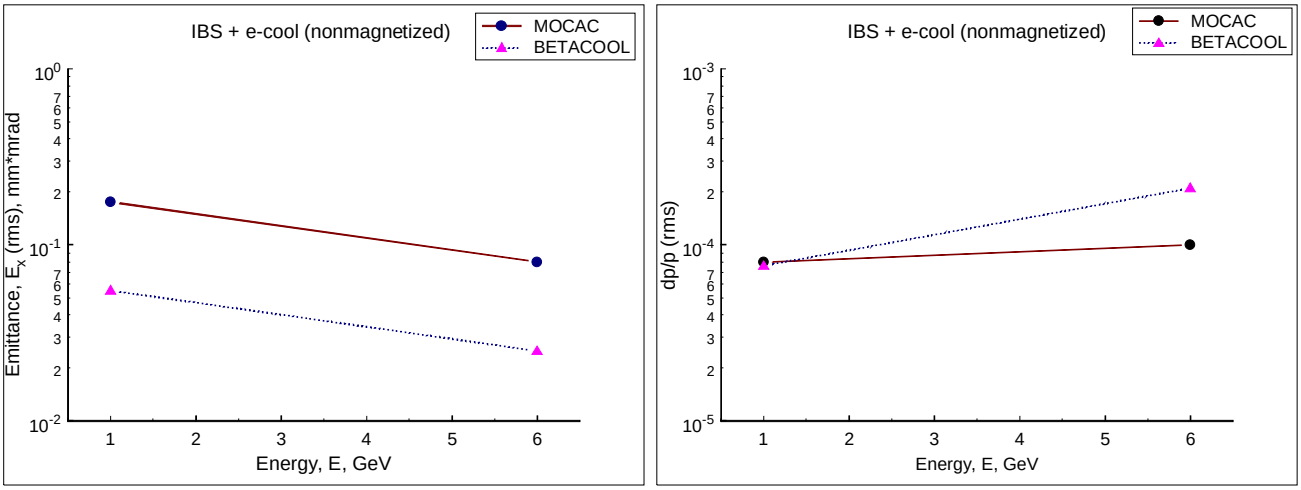

Fig.7 The equilibrium horizontal emittance and momentum spread calculated by MOCAC and BETACOOL codes ('non-magnetized' electron cooling)

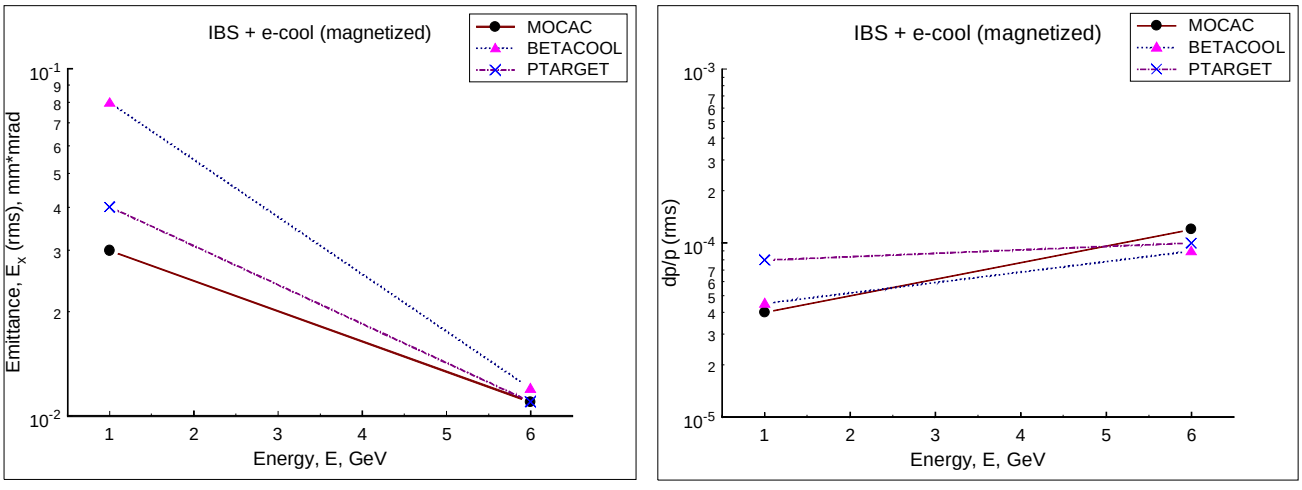

Fig.8 The equilibrium horizontal emittance and momentum spread calculated by MOCAC, BETACOOL and PTARGET codes. ('magnetized'electron cooling)

The next two fig.9,10 show the calculated results at the same cooling condition, but here the IBS and internal target influence on the beam heating. The jet target [15] thickness of 5×10^{15} cm^{-2} is chosen to reach in the HESR the average luminosity of 2×10^{32} $cm^{-2}s^{-1}$. The beta-function both in horizontal and vertical planes at the target was assumed of 1.5 m. One can see that all codes indicate the possibility to have the equilibrium states at the energy of 1 GeV independently on which electron cooling applied (non-magnetized (fig.9) or magnetized (fig.10)). But at the range of high energy (for example 6 GeV) there is no possible at given electron condition to reach the equilibrium beam parameters at least after 2500 s.

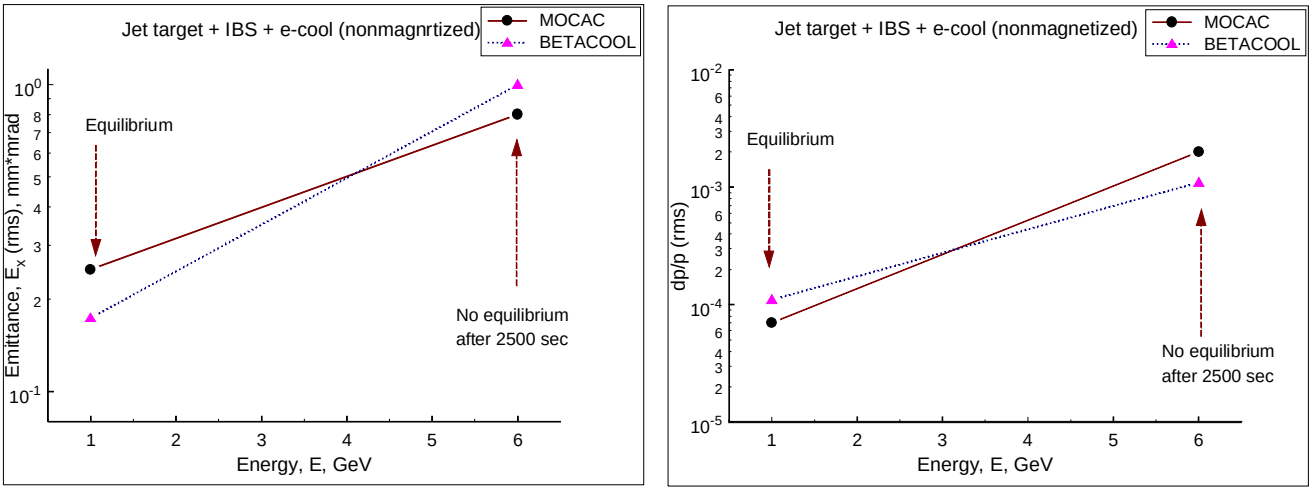

Fig.9 The equilibrium horizontal emittance and momentum spread calculated by MOCAC and BETACOOL codes (non-magnetized electron cooling, $n_e=1\times10^6$ cm^{-3}). The internal jet target thickness is 5×10^{15} cm^{-2}.

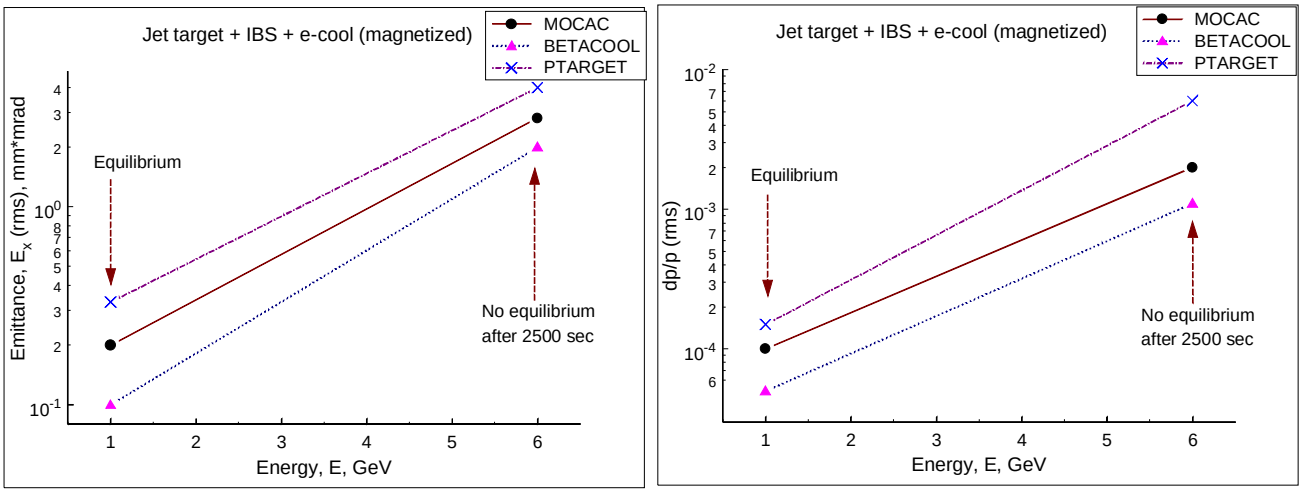

Fig.10 The equilibrium horizontal emittance and momentum spread calculated by MOCAC, BETACOOL and PTARGET codes (magnetized electron cooling, $n_e=1\times10^6$ cm^{-3}). The internal jet target thickness is 5×10^{15} cm^{-2}.

Assuming a balance between cooling and heating rate by IBS and target the equilibrium state must depend on the electron beam intensity which determines the cooling rate. Higher electron density result in an increased cooling rate at higher energy which gives possibility to reach the equilibrium state and at the same time one can obtain lower equilibrium temperature of the antiproton beam at high energy. Calculation by BETACOOL shows that increasing of the electron density to 10^7 cm^{-3} in magnetized case gives equilibrium state only at the energy up to 4 GeV (Fig.11a). In Fig.11b the cooling time, which is necessary to reach the equilibrium parameters plotted in Fig.11a, are shown. To have the equilibrium at more higher energy (up to 14 GeV) the electron density must be increased again at least by factor 4 (Fig.12a,b).

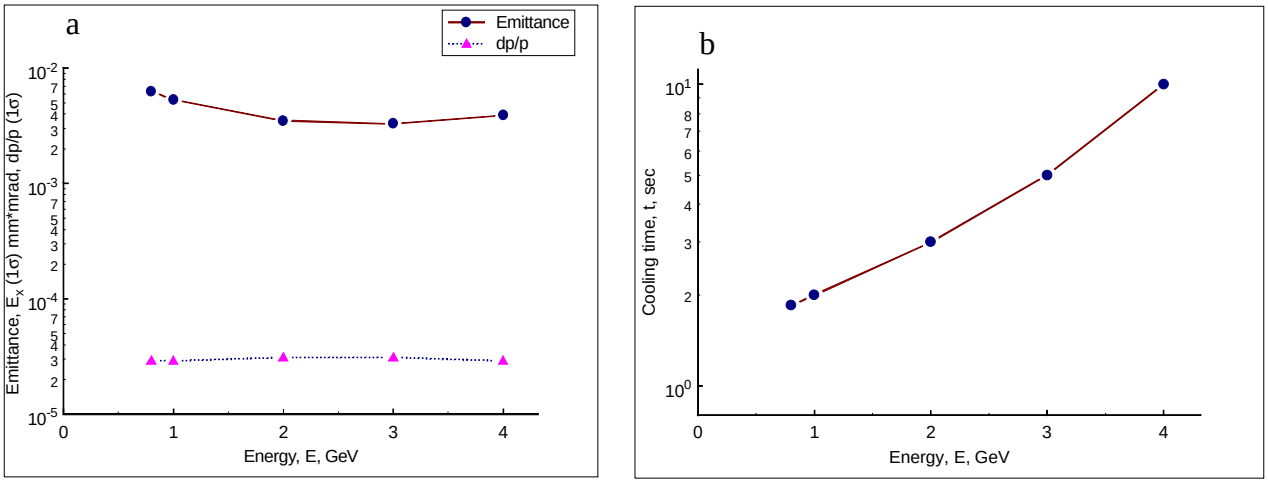

Fig.11 a) The equilibrium horizontal emittance and momentum spread; b) the cooling time calculated by BETACOOL code (magnetized electron cooling, n_e=1×10^7 cm^{-3}).
The internal jet target thickness is 5×10^{15} cm^{-2}.

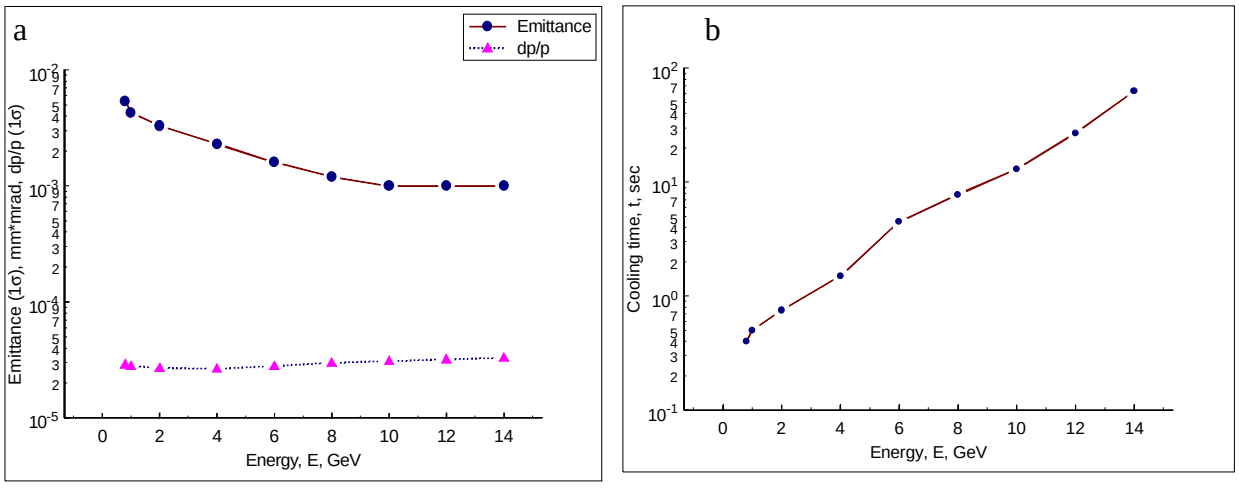

Fig.12 a) The equilibrium horizontal emittance and momentum spread; b) the cooling time calculated by BETACOOL code (magnetized electron cooling, n_e=4×10^7 cm^{-3}).
The internal jet target thickness is 5×10^{15} cm^{-2}.

According to MOCAC simulation the equilibrium state is possible to reach at energy of 6 GeV if the electron density is 2×10^7 cm^{-3}. In Fig.13,14 the evolution beam parameters with a time calculated by MOCAC code are shown for the energy of 1 and 6 GeV respectively. One can see that even at non-magnetized electron cooling with such density the equilibrium state is possible to reach. But in this case the equilibrium temperatures is much higher compare with magnetized electron cooling. As it is seen from fig.9-14 both codes indicate considerable dependence of the quality antiproton beam on the electron density. It should be noted that the transverse emittance usually shows a weaker dependence on the electron density than it for momentum spread.

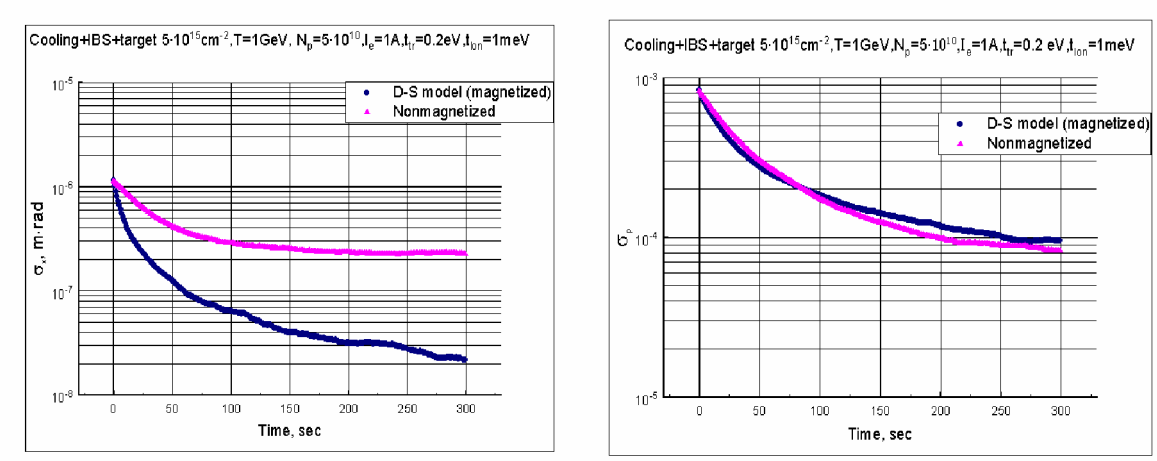

Fig.13 Evolution of the horizontal emittance and momentum spread with a time calculated by MOCAC code for the antiproton energy of 1 GeV ($n_e=2\times10^7$ cm^{-3}). The internal jet target thickness is 5×10^{15} cm^{-2}. (D-S model – Derbenev-Skrinsky model (formulae 2,3))

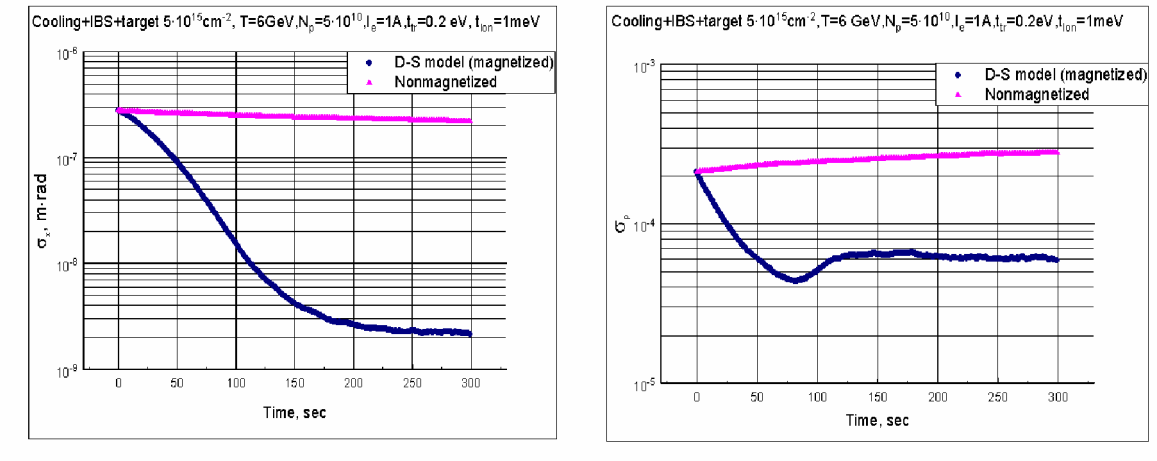

Fig.14 Evolution of the horizontal emittance and momentum spread with a time calculated by MOCAC code for the antiproton energy of 6 GeV ($n_e=2\times10^7$ cm^{-3}). The internal jet target thickness is 5×10^{15} cm^{-2}. (D-S model – Derbenev-Skrinsky model (formulae 2,3))

The similar results were obtained also by PTARGET code, where instead of the jet target the pellet target was applied [16]. The pellets of 30 μm diameter having a speed of 60 m/s move through the circulating beam. According to parameters of the pellets given in [17,18] we assume that there is one pellet in a rectangle of height 0.9 mm and width 2 mm. Tacking into account the area, which is occupied by one pellet, one can easily to calculate for the frozen hydrogen (ρ=0.0708 g/cm^3 density of frozen hydrogen) the number of atoms in one pellet, which is about 6×10^{14} cm^{-2}. This value gives the locale thickness of order 10^{19} cm^{-2} (for diameter of 30 μm). Tacking into account the area, which is occupied by one pellet one can easily to calculate the effective target thickness of 3.3×10^{16} cm^{-2}. If the circulating beam in horizontal plane is matched to the width of the pellet beam (2 mm) and the number of stored particles is 5×10^{10} and circulating frequency is about 1.5×10^{5} s^{-1} the luminosity will be about 3×10^{33} cm^{-2}s^{-1}. According to PTARGET calculation the electron cooling will not be able to suppress the beam heating comes from the target with effective thickness of 3.3×10^{16} cm^{-2} for high energy (more than 2 GeV) even at the electron density of 1×10^{7} cm^{-3}. The effective target thickness can be adjusted to optimum values of order 5×10^{15} cm^{-2} by choosing of the necessary value of the beta function at the target position. Due to larger value of the beta-fuction the pellets will occupy a smaller fraction of the area of the stored beam, this gives increasing of the ratio between the target area and stored beam area that results in the designed value of the effective target thickness of 5×10^{15} cm^{-2}. At such target thickness the electron cooling can provide the acceptable parameters of the equilibrium state for the antiproton energy up to 6 GeV as it is shown in fig.15,16. Here the beta function is about 10 m at the target position. At the same time one can see that at given parameters of the HESR the maximal luminosity will be in range of about 2×10^{32} cm^{-2}s^{-1}.

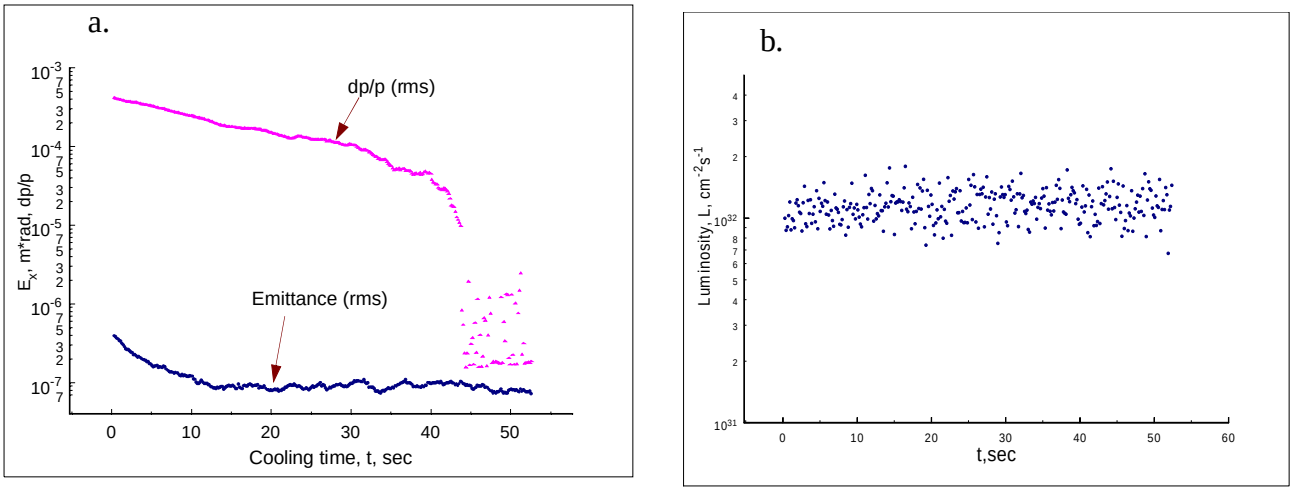

Fig.15 a) The equilibrium horizontal emittance and momentum spread; b) the luminosity calculated by PTARGET code at the energy of 1 GeV (magnetized electron cooling, n_e=10^7 cm^{-3}).The effective pellet target thickness is 5×10^{15} cm^{-2}. Beta-function at the target β_{tr}=10 m

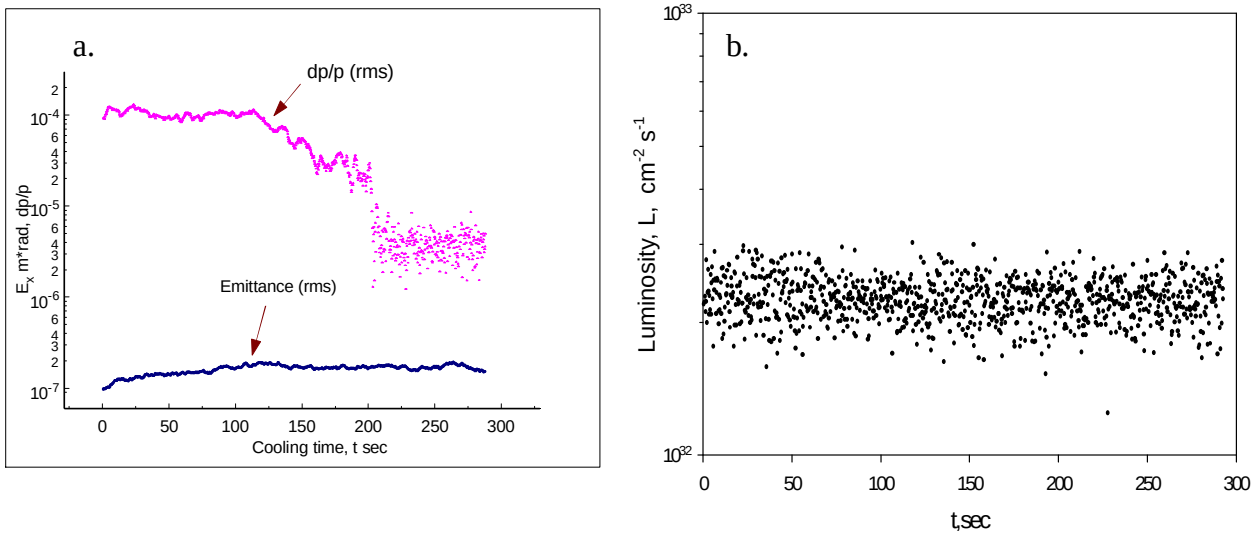

Fig.16 a) The equilibrium horizontal emittance and momentum spread; b) the luminosity calculated by PTARGET code at the energy of 6 GeV (magnetized electron cooling, n_e=1×10^7 cm^{-3}). The effective pellet target thickness is 5×10^{15} cm^{-2}. Beta-function at the target β_{tr}=10 m.

5 CONCLUSION

The numerical simulations of the equilibrium beam states in the HESR have been done by three different codes (BETACOOL, MOCAC, PTARGET), where the different algorithms for calculation of the cooling, IBS and internal target heating are applied. As it was demonstrated the beam quality and luminosity in the HESR will be limited by the capability to suppress by electron cooling the heating processes which are took place in a storage ring due to IBS and an internal target. The maximal luminosity of 2×10^{32} cm^{-2}s^{-1} with equilibrium beam emittance less then of 0.1 mm·mrad and momentum spread better then ±3×10^{-5} can be achievable if the strong cooling will be possible to implement in the HESR for high antiproton energy (in range of 0.8-14.5 GeV). According to calculation, to reach such equilibrium state in case of using of a internal jet target with thickness of 5×10^{15} cm^{-2} one has to apply the electron cooling, where the electron density if about 4×10^7 cm^{-3}. Some advantages gives us the applying of the pellet target with the same effective target thickness. In this case the required electron density can be 1×10^7 cm^{-3} (up to 6 GeV?).

Further developments are required the achievement of strong electron cooling, which can only be achieved by so called magnetized electron beam. This can be reached if the average distance between electrons $r_{av} \cong n_e^{1/3}$, with the electron density n_e, is large compared to the radius of cyclotron motion in the longitudinal magnetic guiding field. For the mentioned electron density of 1×10^7 cm^{-3} and an energy $\gamma \cong 15$ a longitudinal magnetic field $B \geq 0.5$ T along the entire interaction region of ion and electron beam (up to 30 m) is required. The parallelled of the magnetic field in the cooling section, which is mandatory for fast cooling, should not exceed a value of $B_\perp / B_\parallel \leq 1\times10^{-5}$.

Furthermore, to make full using of the increased magnetized cooling force the pre-cooled antiproton beam with normalised emittance of 2 mm·mrad in both plane and momentum spread of ±4×10^{-4} (at 1 GeV) is required for injection in the HESR.

REFERENCES

[1] "An International Accelerator Facility for Beams of Ions and Antiprotons", Conceptual Design Report, GSI-Darmstadt, November 2001 (see www.gsi.de)

[2] B. Franzke et.al, Conceptual design of a facility for internal target experiment with antiprotons up to 15 GeV/c. Proc. Of the 8th Europ.Part.Acc.Conf., Paris, 2002, p.575.

[3] A.Sidorin, I.Meshkov, Cooling of stored beam after interaction with internal target. Proc. of International Workshop on Rare Isotope Physics at Storage Rings, Hirschegg, Austria, February, 2002.

[4] I.N.Meshkov, Electron cooling with a circulating electron beam in GeV energy range, NIM A441 (2000), p.255

[5] A.E.Bolshakov et al, "Numerical Code for Monte Carlo Simulation of Ion Storage", Conf. on Space Charge Dominated Beam Physics for HIF, Saitama, Japan, (AIP Proceedings 480), p.31, 1998.

[6] A. E. Bolshakov et al, "Modeling of Electron Cooling by Monte Carlo Method", Proc. of Symposium on Electron Cooling, Bad Honnef, Germany, 2001.(will be published)

[7] I.N.Meshkov, Electron cooling: Status and perspectives. Phys.Part.Nucl.25(6) (1994) 631

[8] J.Bosser, Electron cooling, CAS CERN95-06, CERN, Geneva, 1995, p.673

[9] M.Steck at al., Proc. Of the 3rd Europ.Part.Acc.Conf. Berlin 1992, p.827

[10] M.Martini 'Intrabeam scattering in the ACOOL-AA machines. CERN PS/84-9 AA, Geneva, May, 1984.

[11] A.Piwinski, Proc. of the 9th Int. Conf. On High Energy Accelerators, p.105,1974.

[12] A.Piwinski, ' Intra-Beam Scattering', CAS-CERN Accelerator school,16-27 Sep.1991.

[13]B.Hochadel at al. Studies of intrabeam scattering at the TSR, CERN 94-03, Geneva 1994.

[14]F.Hintenberg, D.Prasuhn, Analysis of internal target effects in light ion storage rings. NIM A279(1989) p.413.

[15] M.Macri, Gas jet internal targets, CERN Accelerator school, Report CERN 84-15, Geneva,1983

[16] B.Trostell, Vacuum injection of hydrogen micro-sphere beams, NIM A362 (1995) p.41

[17] C.Ekström at al. Hydrogen pellet targets for circulating particle beams, NIM A371(1996) p.572

[18] C.Ekström, D.Reistad, CELSIUM as an η factory, Proc. Of the 5th Europ. Part. Acc. Conf, Barselona, 1996.

Appendix A

The simulation of the beam dynamic in the HESR by MOCAC code.

Beta function in the electron cooling section.

To find out the optimal value of the beta function in the electron cooling section the beam dynamic of the antiproton beam in the HESR has been calculated by MOCAC code. In Fig.1-6 the results of simulation for three antiproton energy (1 GeV, 8 GeV, 14 GeV) are shown. The emittance and momentum spread versus time calculated without taking into account the heating of the beam on the target are shown in Fig.1. In Fig.2 the same calculations are shown with heating of the beam on the internal jet target. The parameters of the electron beam, which have been used in calculation, are the next: the electron beam radius is 1 mm, the electron current is 1 A, the longitudinal magnet field is 5 kGs, the length of electron cooling section is 30 m. As a initial parameters of antiproton beam that are injected in the HESR we consider that the normalised emittance is 4 mm*mrad and momentum spread is $\pm 5\times10^{-4}$ at energy 3 GeV. To have the desirable value of the average luminosity the internal jet target thickness is 5×10^{15} cm^{-2}.

Applying if the RF for compensation of the mean energy losses.

Due to interaction of the antiproton beam with the internal target one should expect the mean energy losses, which can be calculated by the Bethe-Bloch formula [1]

$$-\bar{\varepsilon} = 2\xi \ln\left(\frac{E_{\max}}{I} - \beta^2\right),$$

where the parameters E_{max} and ξ are defined in our notation reads in section 2.3, I is the mean ionization potential ($I=Z_{tr}^{0.9}\times16$ eV), $\beta=v/c$. For our target thickness and beam energy this value is about 0.02 eV. The calculation taking account the mean losses, energy straggling per target traversal and electron cooling has been done. In Fig.3 one can see the evolution of the horizontal emittance and momentum spread with a time in the HESR at different regime. As it is seen from fig.3 the electron cooling can not compensate the mean energy loss. This losses can be made negligible by applying some RF cavity, where a large bucket size is adjusted in longitudinal phase space. The necessary condition for RF can be obtained by comparing the rms width of the bunch length and the maximum relative deviation of the bucket.

Equilibrium beam parameters.

The results of calculation of the equilibrium states in the HESR are plopped in Fig.4a. The required cooling times to reach such equilibrium states are shown in fig4b. These results were obtained assuming that the value of the beta function in the e-cool is 200 m in both horizontal and vertical planes. One can see that at the initial time (before starting of cooling) the antiproton beam size is much larger then the electron beam (a_e=3 mm). For example at the energy 1 GeV beam radius is : $a_b=(\varepsilon_n\beta_{cool}/(\beta\gamma))^{1/2}$=20 mm ($\varepsilon_n$=4 mm*mrad is normalized emittance). However, as it is seen from fig.4, the electron cooling works effectively due to high electron density $n_e=6.6\times10^9$ cm^{-3} that corresponds to the effective electron density of 2×10^7 cm^{-3}.

[1] Particle Data Group, Phys.Lett. B204 (1988) 1.

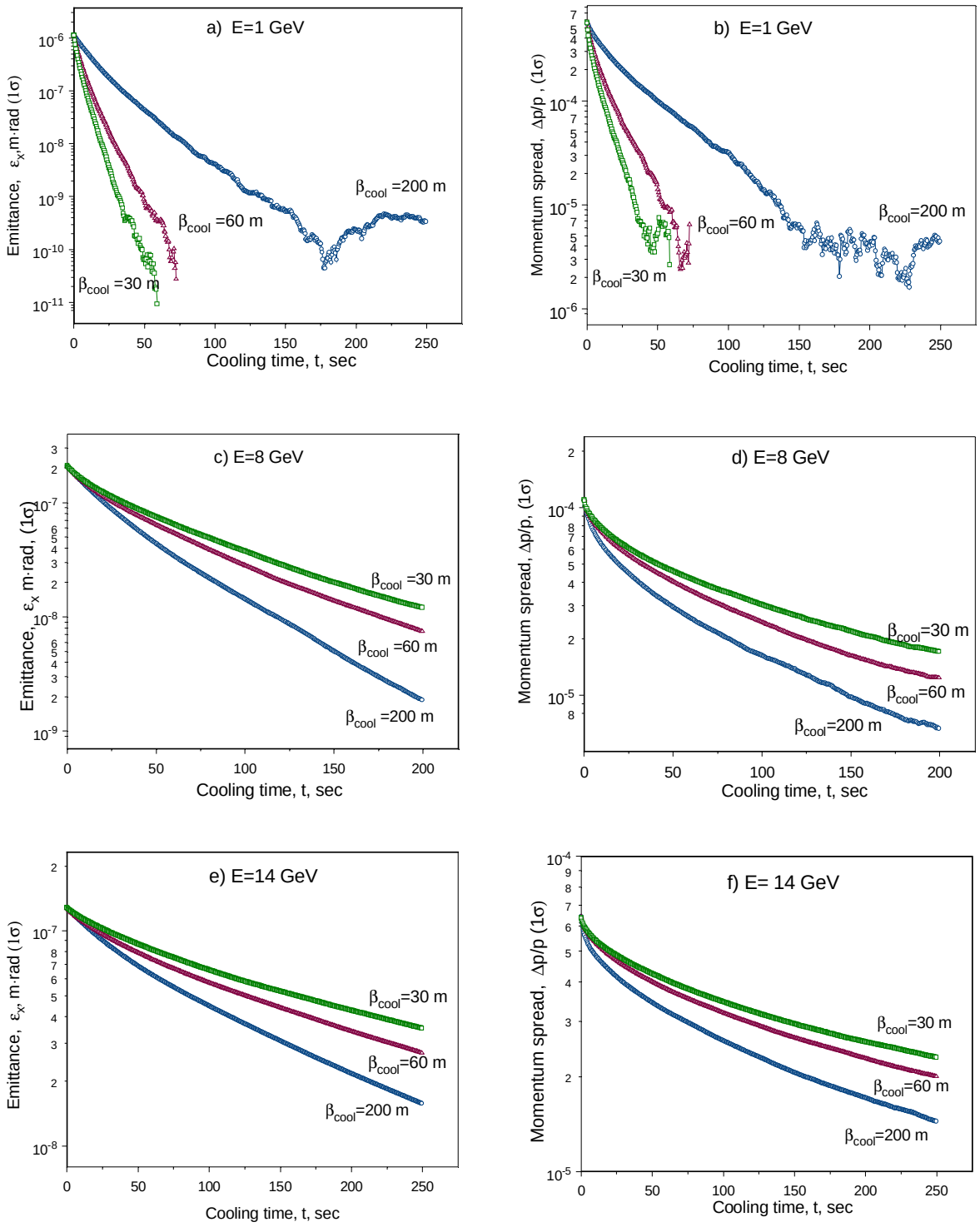

Fig.1 Evolution of the horizontal emittance and the momentum spread with a time for different values of the beta-function (β_{cool}) in the electron cooling section and for different energy of antiprotons. The radius of the electron beam a_e=1 mm, electron current I=1 A, the number of the antiproton N=5×10^{10}. There is no influence of the internal target.

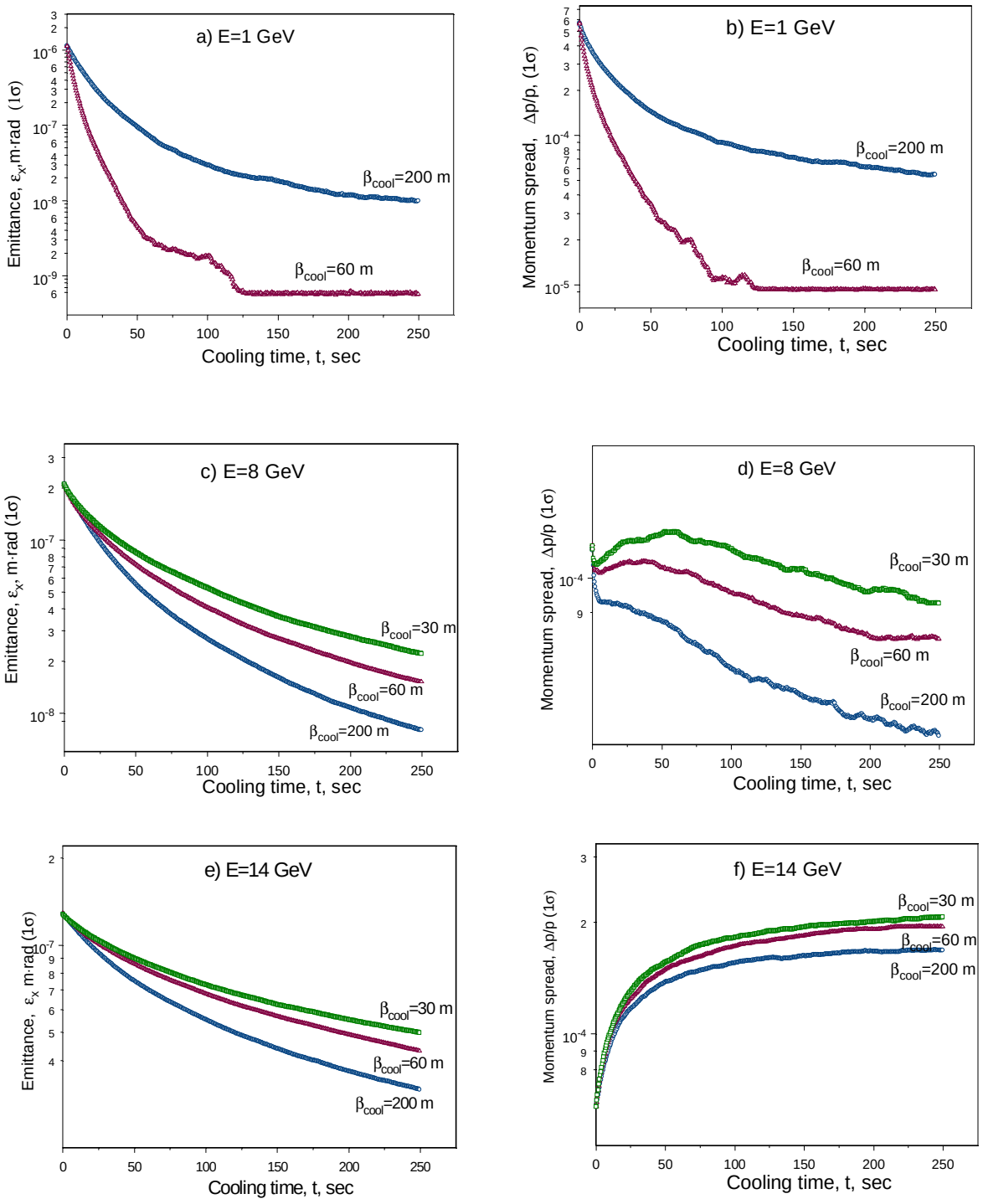

Fig.2 Evolution of the horizontal emittance and the momentum spread with a time for different values of the beta-function (β_{cool}) in the electron cooling section and for different energy of antiprotons. The radius of the electron beam a_e=1 mm, electron current I=1 A, the number of the antiproton N=5×10^{10}. There is influence of the internal jet target with a thickness of 5×10^{15} cm^{-2}.

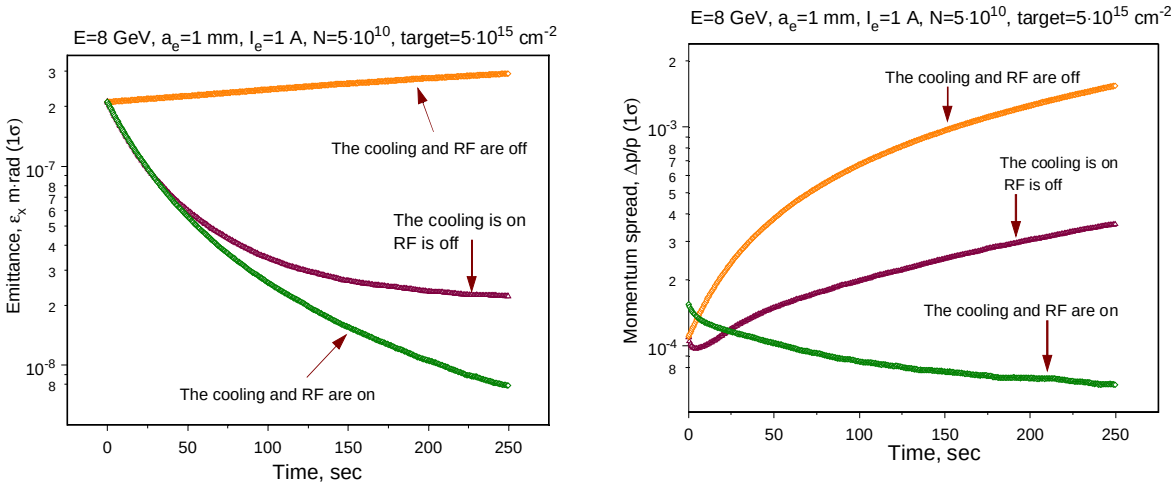

Fig.3 Evolution of the horizontal emittance and the momentum spread with a time applying the RF cavity.

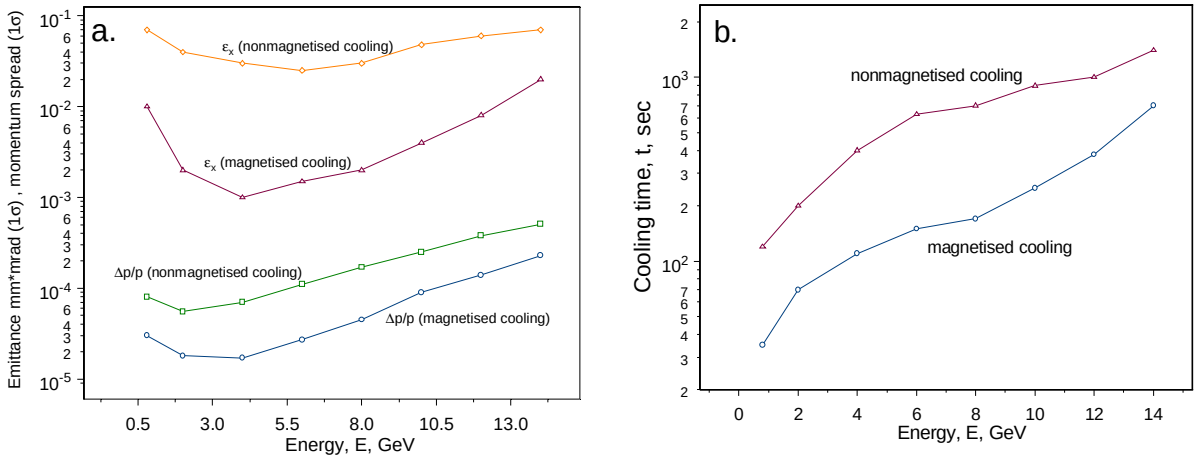

Fig.4 a) The equilibrium horizontal emittance and momentum spread; b) the cooling time, which is needed to reach the equilibrium states. The a_e radius of the electron beam is 3 mm, the I electron current is 1 A, the N number of the antiprotons is 5×10^{10}, the thickness of the internal jet target is 5×10^{15} cm^{-2}.

Condition for a compensation of the average energy losses with the electron cooling.

As it was shown in Fig.3 for compensation of the average energy losses on the internal jet target one has to apply a RF cavity, which should add every turn about of 0.02 eV to an energy of antiproton beam. This value is rather small and, in principle, at certain condition the electron cooling can be used instead of the rf cavity to compensate this energy losses . Let us assume that an antiproton beam are precooled and about size of the electron beam and equal of 3 mm. For different electron current in fig.5 the evolution of the transversal emttances and momentum spread with a time are shown. One can see that at the electron current of about 0.1 A (n_e=7.4×10^7 cm^{-3}) there are no growth of the momentum spread and blow up of the emittances at any time.

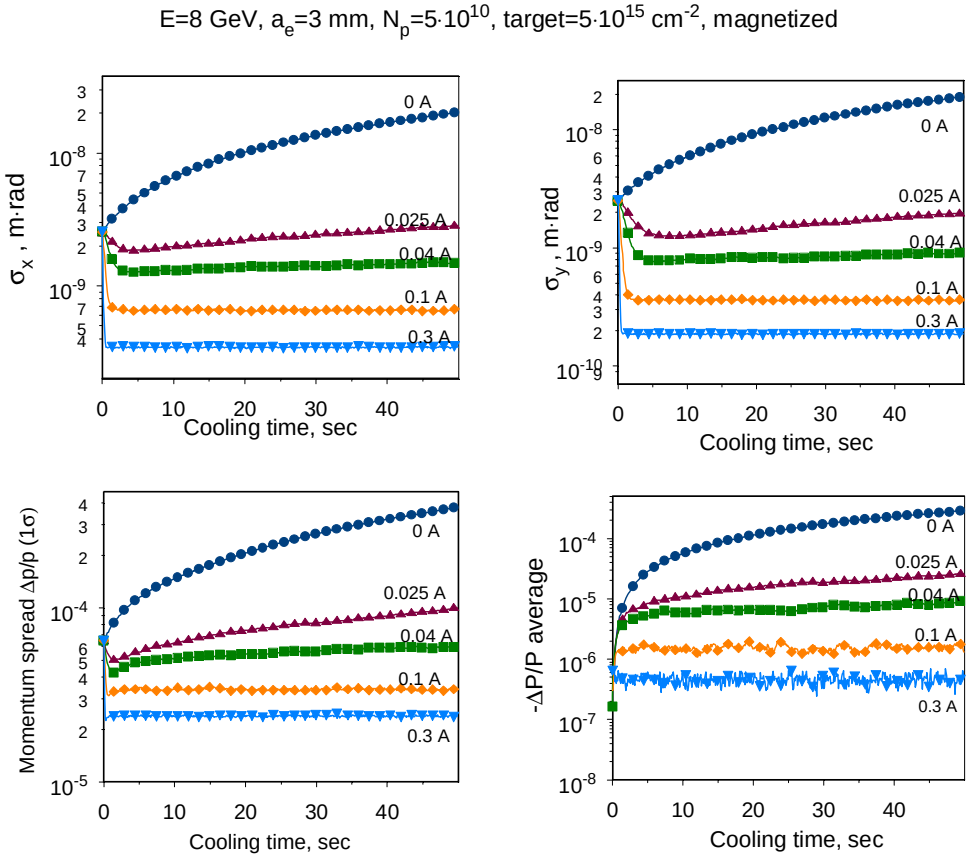

Fig.5 Evolution of the beam parameters with a time in the HESR.